

Building damage assessment using a single post-earthquake PolSAR image: a case of the 2010 Yushu earthquake

Wei Zhai¹, Wenhao Zeng^{1,*}

¹ Monitoring Center, Gansu Earthquake Administration, 730000, Lanzhou, Gansu, China

The corresponding author's e-mail: zwxzzdsyhq@163.com

Abstract. Earthquakes are one of the most destructive natural disasters. Efficiently and quickly acquiring building earthquake damage information can help to reduce the casualties after an earthquake. In this paper, building damage information is extracted using a single post-earthquake PolSAR image. In PolSAR images, since the undamaged oriented buildings characterized by volume scattering with weaker scattering power are very similar to collapsed buildings, the collapsed buildings are difficult to extract accurately. In this paper, the difference in the relative contribution change rate of scattering components before and after polarization orientation angle (POA) compensation is proposed to enhance the difference between collapsed buildings and oriented buildings, in order that the collapsed buildings can be extracted more accurately. The “4.14” Yushu earthquake, which occurred in Yushu County, Qinghai province of China, is used as the case study to test the proposed method, and an airborne high-resolution PolSAR image of the urban region of Yushu County is used in the experiment. The experimental results show that the accuracy of building damage information extraction can be improved by the use of the proposed method, compared with the traditional polarimetric classification.

1. Introduction

Earthquakes can give rise to great damage to life and property. In an earthquake, most of the casualties are caused by collapsed buildings, so building damage information extraction is the main task of earthquake damage information investigation. After an earthquake, the collapsed building information should be acquired in a timely manner, and can be used to guide the effective implementation of the emergency rescue, which is crucial for the reduction of casualties^[1]. Radar is not affected by weather and climate, and can obtain images in bad weather and even at night^[2], because of its strong penetrative power, so it has become a reliable remote sensing data source for acquiring the damage information of earthquake-stricken areas. Compared to single-polarization synthetic aperture radar (SAR), fully polarimetric SAR (PolSAR) is capable of recording the backward scattering information in four kinds of polarization mode, which contain much more information and are more helpful for understanding the characteristics of ground objects^[3,4].

Most of the studies about the disaster investigation using PolSAR data were carried out mainly based on the changes of polarimetric features between pre- and post-earthquake using multitemporal PolSAR data^[5-9]. However, archived pre-event PolSAR images matched with the post-event images are often difficult to obtain, and the registration of the pre- and post-event PolSAR images also costs



time and manpower. Therefore, earthquake damage assessment using only a single post-earthquake PolSAR image has attracted the attention of more and more researchers. Guo et al.^[10] and Li et al.^[11] introduced the circular polarization correlation coefficient ρ and proposed the H - α - ρ method to extract collapsed building information using Radarsat-2 polarimetric data after the “4.14” Yushu earthquake. Zhao et al.^[12] introduced the texture parameter of *homogeneity* to improve the H - α - ρ method using high-resolution airborne PolSAR data. Shen et al.^[13] used the method of image retrieval based on feature template matching to extract the collapsed building information.

This study is devoted to extracting building damage information using a single post-earthquake PolSAR image. The collapsed buildings are mainly characterized by volume scattering due to the destruction of the building structure. The uncollapsed oriented buildings which are not parallel to the flight pass of the radar can cause polarization orientation angle (POA) shift, so that volume scattering becomes the dominant scattering mechanism. If the traditional polarimetric classification methods are used to extract the collapsed buildings, the oriented buildings can be easily misclassified as collapsed buildings, and the building collapse rate is likely to be overestimated, especially in built-up areas containing many oriented buildings. In view of this, the difference in the change rate of the relative contributions of double-bounce scattering and volume scattering, $CR_{Dbl-Vol}$, is introduced to help to distinguish the two types of buildings. The experiments show that the building damage assessment accuracy can be improved using the method proposed in this paper.

2. Methodology

2.1. Analysis of building scattering components in earthquake-stricken areas

The buildings of earthquake-stricken areas are divided into three classes in this paper, based on the characteristics of the PolSAR images: collapsed buildings, parallel buildings, and oriented buildings. The scattering power of parallel buildings is particularly strong because they form a dihedral structure with the ground, but the scattering power of oriented buildings is as weak as the collapsed buildings. Compensating the POA shift induced by the polarization basis being rotated can enhance the double-bounce scattering power of the oriented buildings. The details about the scheme of POA compensation can be found in^[14]. In order to comprehend the changes in the scattering mechanism after POA compensation for the three kinds of buildings, the four scattering components generated from Yamaguchi four-component decomposition^[15], before and after POA compensation, are analyzed in this section.

The relative contributions of the four components of the three kinds of building samples selected in Fig. 4, before and after POA compensation, are shown in Fig. 1. As can be seen in Fig. 1, the dominant scattering component of the parallel buildings is double-bounce scattering, and the oriented buildings and the collapsed buildings are dominated by the volume scattering component. Before and after POA compensation, the relative contributions of each scattering component for the parallel buildings basically remain the same, while the relative contribution of double-bounce scattering for the oriented buildings more than doubles, and the relative contribution of volume scattering significantly decreases. In addition, for the collapsed buildings, the relative contribution of double-bounce scattering also increases, but the increase is less than for the oriented buildings, and the decrease in the relative contribution of volume scattering is very small. In conclusion, for the oriented buildings, the scheme of POA compensation can greatly improve the relative contribution of the double-bounce scattering component, and can significantly reduce the relative contribution of the volume scattering component.

2.2. $CR_{Dbl-Vol}$

Inspired by the conclusion deduced from Fig. 1, the change rates of the relative contribution before and after POA compensation (CR , for short) for the double-bounce scattering component and the volume scattering component are shown in Fig. 2. As can be seen from Fig. 2, the CR for the double-bounce scattering component (CR_{Dbl} , for short) of the oriented buildings is more than twice as large as

that of the collapsed buildings, and the amplitude of the CR for the volume scattering component (CR_{Vol} , for short) of oriented buildings is also larger than that of collapsed buildings. In view of this, the difference of the CR between the double-bounce and volume scattering components is defined as:

$$CR_{Dbl-Vol} = \frac{Dbl_{afterPAC} - Dbl_{beforePAC}}{Dbl_{beforePAC}} - \frac{Vol_{afterPAC} - Vol_{beforePAC}}{Vol_{beforePAC}} \quad (1)$$

where $Dbl_{beforePAC}$ denotes the relative contribution of the double-bounce scattering component before POA compensation;

$Dbl_{afterPAC}$ is the relative contribution of the double-bounce scattering component after POA compensation.

$Vol_{beforePAC}$ denotes the relative contribution of the volume scattering component before POA compensation;

$Vol_{afterPAC}$ is the relative contribution of the volume scattering component after POA compensation.

$CR_{Dbl-Vol}$ is also shown in Fig. 2. The difference in $CR_{Dbl-Vol}$ between collapsed buildings and oriented buildings is more distinct than the difference in CR_{Dbl} and in CR_{Vol} . The difference in $CR_{Dbl-Vol}$ of oriented buildings is much greater than that of collapsed buildings.

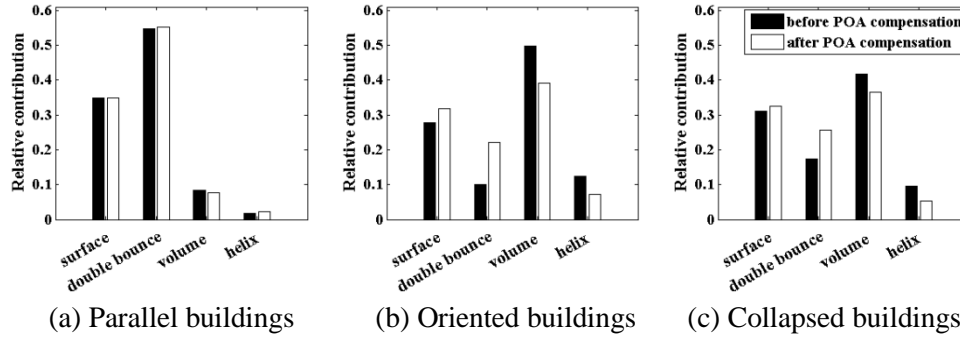


Figure 1. Relative contribution of the different scattering mechanisms of the three kinds of buildings before and after POA compensation

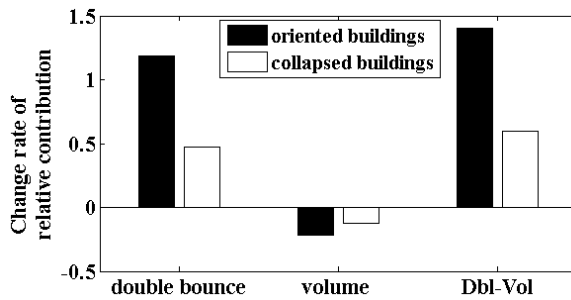


Figure 2. Change rate of the relative contribution of the different scattering mechanisms for the oriented and collapsed buildings before and after POA compensation.

As can be seen from Fig. 1, the relative contribution of the double-bounce scattering component of the oriented buildings after POA compensation cannot be increased as much as for the parallel buildings. Therefore, the classification result of the oriented and collapsed buildings generated from the Wishart supervised classification performed on the PolSAR data after POA compensation is still not very accurate. However, the difference in $CR_{Dbl-Vol}$ between the oriented buildings and the collapsed buildings can be used to distinguish the two kinds of buildings, and to correct the results of the two kinds of buildings obtained from Wishart supervised classification, so as to improve the accuracy of the collapsed building extraction. Using $CR_{Dbl-Vol}$ to separate the two kinds of buildings can be expressed as:

$$\begin{cases} \text{if } CR_{Dbl-Vol} > \varepsilon, x \in \text{oriented buildings} \\ \text{if } CR_{Dbl-Vol} \leq \varepsilon, x \in \text{collapsed buildings} \end{cases} \quad (2)$$

where ε is the threshold value of $CR_{Dbl-Vol}$ set according to experiment, and x is a pixel of the PolSAR image.

3. Building earthquake damage information extraction

The process of building damage information extraction is shown in Fig. 3. Firstly, POA compensation is performed on the PolSAR data after preprocessing, and the new $[C]$ matrix is obtained. Secondly, according to the case study selected in this paper, the ground objects in the earthquake-stricken area are classified as bare areas, collapsed buildings, parallel buildings, and oriented buildings, using the Wishart supervised classification^[17] implemented on the PolSAR data after PolSAR compensation. Thirdly, the values of $CR_{Dbl-Vol}$ of the collapsed buildings and oriented buildings are calculated, and the threshold value ε is set to separate the two kinds of buildings according to the difference in $CR_{Dbl-Vol}$ between the collapsed buildings and the oriented buildings, as shown in Fig. 2. In this way, the new class centers for the two kinds of buildings are obtained. The clustering and iteration using the complex Wishart classifier needs to be carried out again to update the new class centers. After this, the two classes of collapsed buildings and oriented buildings generated from the Wishart supervised classification are corrected. Finally, the parallel buildings and the oriented buildings are combined as the undamaged buildings. The building collapse rate (BCR) is calculated at the scale of the city block, which is defined as the ratio of the collapsed buildings to the total buildings of one block. The damage levels of the buildings are divided into slight, moderate, and serious damage levels according to the threshold values of the BCR of each city block.

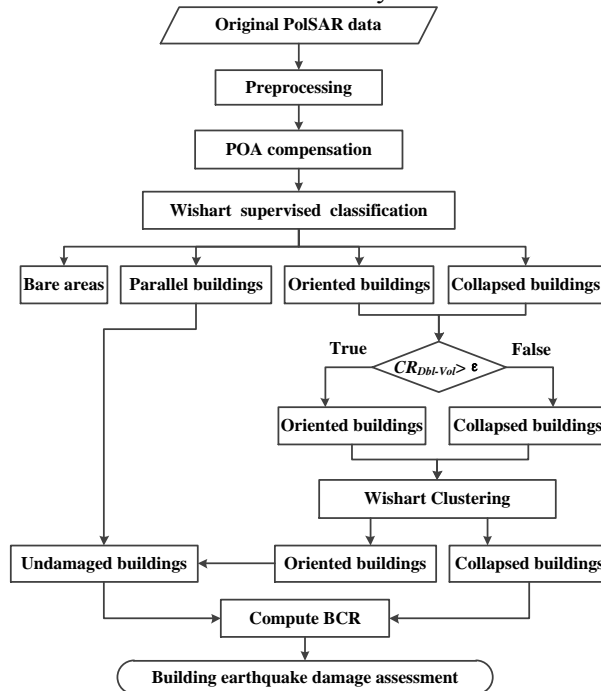


Figure 3. Experimental flow chart of building earthquake damage information extraction

4. Experiment and analysis

4.1. Experimental Data

In this paper, the selected case study is the Yushu earthquake of magnitude 7.1 that occurred in Yushu County, Qinghai province, China, on April 14, 2010. The location of the epicenter was 33.1°N and 96.6°E. There were many collapsed buildings and more than 2600 people died in the earthquake. The direct economic losses amounted to more than 22 billion CNY. The study area is the urban region of Yushu County. The vegetation is very sparse and low-level in this urban region, so it was ignored in the experiment. The buildings are mainly low-rise rural residential buildings in Yushu County.

The experimental data are the airborne high-resolution PolSAR image acquired one day after the earthquake in the P-band by the Chinese airborne SAR mapping system (SARMapper). Both the range resolution and azimuth resolution are approximately 1 m. The flight pass was in an east–west horizontal direction. The Pauli RGB image is shown in Fig. 4 with the size of 8192×4384 pixels. In the PolSAR data, the mountains surrounding the urban area were removed by masking, and only the urban region was kept. The whole urban region was divided into 72 city blocks by roads and according to the similarity of the built-up patches. The earthquake damage assessment reference information is shown in Fig. 5. The building damage levels of the 72 city blocks were divided into slight, moderate, and serious damage levels.

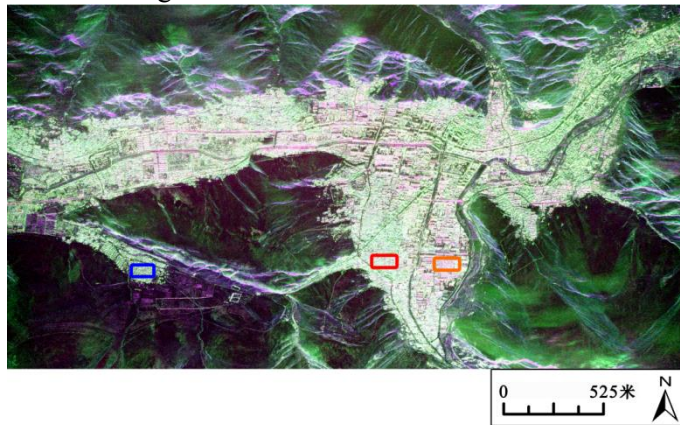


Figure 4. Pauli RGB color composite image of PolSAR data of Yushu County, with red ($|HH-VV|$), green ($|HV|$), and blue ($|HH+VV|$). The areas in red, blue, and orange boxes are the samples of the collapsed buildings, oriented building, and parallel buildings, respectively.

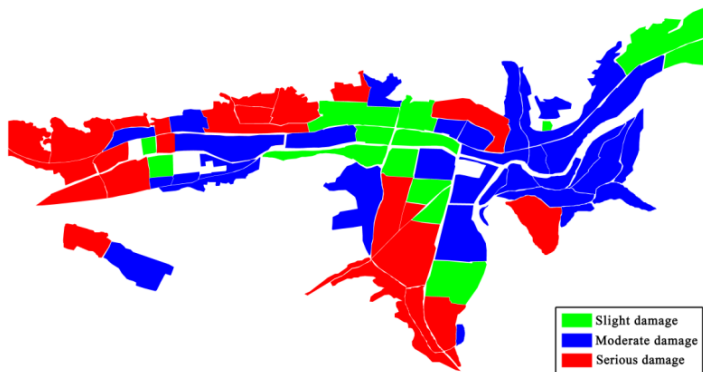


Figure 5. Reference map of the building earthquake damage information at the city block scale in the Yushu urban region.

4.2. Experimental Results

According to the process of building earthquake damage information extraction shown in Fig. 3, the Wishart supervised classification method was performed on the PolSAR data after POA compensation. We then calculated the $CR_{Dbl-Vol}$ for all of the samples of oriented buildings and the collapsed buildings generated from the Wishart supervised classification, and set the threshold value ε as 0.7 according to the difference shown in Fig. 2. The two kinds of buildings were reclassified based on Eq. (2), as described in Section 2.2, and clustering based on the Wishart distance was carried out. The final classification results of the oriented buildings and the collapsed buildings were obtained. The oriented buildings together with the parallel buildings were considered to be the undamaged buildings.

The results of extracting the collapsed buildings, the undamaged buildings, and the non-buildings are shown in Fig. 6, in which the red areas are the collapsed buildings, the green areas denote the undamaged buildings, and the blue areas correspond to the non-buildings. The BCR of each block was calculated, and the building damage levels were set as:

$$\left\{ \begin{array}{l} \text{if } BCR \leq 0.2, \text{ the block } \in \text{slight damage} \\ \text{if } 0.2 < BCR \leq 0.5, \text{ the block } \in \text{moderate damage} \\ \text{if } BCR > 0.5, \text{ the block } \in \text{serious damage} \end{array} \right. \quad (4)$$

The map of building damage levels for the whole urban region at the block scale is shown in Fig. 7, and the accuracy evaluation of the experimental results is shown in Table 1 by reference to Fig. 5. For comparison, the results of both the proposed method and the method using Wishart supervised classification directly without POA compensation and $CR_{Dbl-Vol}$, which is termed direct Wishart supervised classification (DWSC), are listed in Table 1.

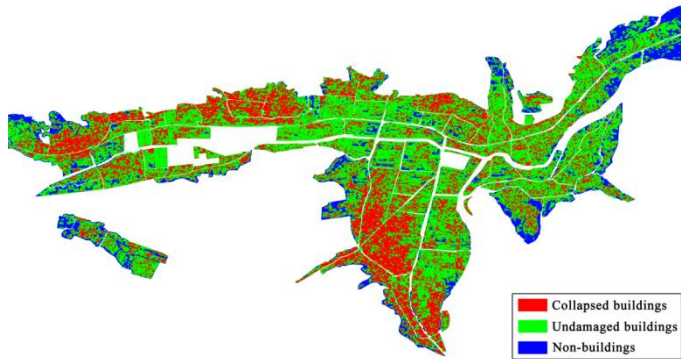


Figure 6. Experimental results distribution map of the collapsed buildings, the undamaged buildings, and the non-buildings in the earthquake-stricken urban area of Yushu County.

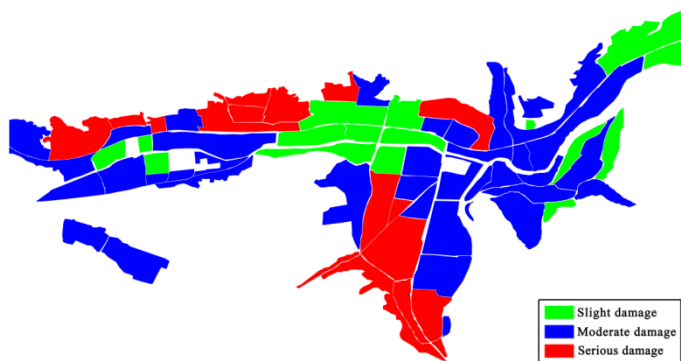


Figure 7. Experimental results map of the building damage levels at the block scale in the Yushu urban region.

Table 1. Accuracy evaluation of the earthquake damage information extraction of the two methods

		The proposed method			DWSC		
		(Experiment)			(Experiment)		
		SLD	MOD	SED	SLD	MOD	SED
		(No. of blocks)					
(Reference)	SLD	11	3	0	9	3	2
	MOD	4	29	0	3	22	8
	SED	1	7	17	0	4	21
		OA: 79.2%			OA: 72.2%		

4.3. Discussion and analysis

As can be seen from Table 1, the overall accuracy of the building earthquake damage information extraction was increased by 7% using the proposed method compared to the DWSC method. There were actually 25 blocks, and 17 blocks were extracted using the proposed method, but 31 blocks were extracted by the DWSC method. Therefore, the proposed method can effectively reduce the overestimation of building earthquake damage. Most of the misclassification situations were those of the slight damage level or the serious damage level being misclassified as the moderate damage level,

and the moderate damage level being misclassified as the slight damage level. In other words, the misclassification of the damage level only spanned one level, and there was only one block of serious damage misclassified as the slight damage level. In short, for the 15 misclassified blocks, the main situation of misclassification involved reduced damage levels.

Although POA compensation can enhance the double-bounce scattering power of oriented buildings, the dominant scattering mechanism of oriented buildings is still volume scattering. Therefore, there are still many oriented buildings and collapsed buildings mixed up with each other in the classification results of the Wishart supervised classification performed on the PolSAR data after POA compensation. Accordingly, the difference in $CR_{Dbl-Vol}$ between oriented buildings and collapsed buildings is used to correct the results of the Wishart supervised classification.

However, the correction can result in the oriented buildings being detected too much and can result in overestimation of the undamaged buildings. This is influenced by the selection of the $CR_{Dbl-Vol}$ threshold value ε for separating oriented buildings and collapsed buildings. In addition, due to the fact that some residual walls of the collapsed buildings form a dihedral structure with the ground, some collapsed building areas also have high double-bounce scattering power, and these areas are easily misclassified as undamaged parallel buildings. In the collapsed building areas, the double-bounce scattering power of some oriented residual walls is increased after POA compensation, and these walls may also be misclassified as parallel buildings. These are the causes of the overestimation of the undamaged buildings.

The overestimation of the undamaged buildings gives rise to a reduction in the building damage level, and the identification accuracy of the blocks with the serious damage level is reduced. However, the identification accuracy of the blocks with the slight damage level and moderate damage level is generally improved, and the overall accuracy is improved.

5. Conclusion

In this paper, building earthquake damage information has been extracted using a single post-event PolSAR image. Because the characteristics of oriented buildings are very similar to the collapsed buildings in PolSAR images, and the double-bounce scattering power of oriented buildings is weak, the scheme of POA compensation is performed on the PolSAR image to enhance the double-bounce scattering power of the oriented buildings. Although the scattering power of oriented buildings in the PolSAR image after POA compensation is increased, the dominant scattering mechanism of oriented buildings is still volume scattering. Therefore, the results of the Wishart supervised classification are not very accurate and need to be improved. Through analyzing the changes in the scattering mechanism before and after POA compensation for the three kinds of buildings, we found that the increase in the amount of double-bounce scattering component and the reduction in the amplitude of the volume scattering component of the oriented buildings are greater than for the collapsed buildings. Accordingly, the parameter of $CR_{Dbl-Vol}$ is proposed to further distinguish the oriented buildings from the collapsed buildings. Therefore, the significant difference in $CR_{Dbl-Vol}$ between collapsed buildings and oriented buildings is used to correct the results of the Wishart supervised classification for the two kinds of buildings, and the collapsed building extraction accuracy is improved. In a comparison with the DWSC method, it was found that the proposed method can improve the accuracy of building earthquake damage assessment.

Acknowledgements

This work was supported by the Earthquake Science and Technology Development Fund Program of Lanzhou Earthquake Research Institute, China Earthquake Administration (2015M02); the Object-oriented High Trusted SAR Processing System of the National 863 Subject Program; and the Airborne Multiband Polarimetric Interferometric SAR Mapping System of the National Major Surveying and Mapping Science and Technology Special Program. We would also like to thank the anonymous reviewers for their advice on improving the quality of this paper.

References

- [1] Zhai W., Shen H.F., Huang C.L., Pei W.S., 2016. Building Earthquake Damage Information Extraction from a Single Post-Earthquake PolSAR Image. *Remote Sens*, 8(3), 171.
- [2] Gamba P., Dell'Acqua F., Trianni G., 2007. Rapid Damage Detection in the Bam Area Using Multitemporal SAR and Exploiting Ancillary Data. *IEEE Trans Geosci Remote Sens*, 45(6), pp. 1582-1589.
- [3] Zhai W., Shen H.F., Huang C.L., Pei W.S., 2016. Fusion of polarimetric and texture information for urban building extraction from fully polarimetric SAR imagery. *Remote Sens Lett*, 7(1), pp. 31-40.
- [4] Zhai W., Huang C.L., 2016. Fast building damage mapping using a single post-earthquake PolSAR image: a case study of the 2010 Yushu earthquake. *Earth Planets Space*, 68(1), 1.
- [5] Yamaguchi Y., 2012. Disaster Monitoring by Fully Polarimetric SAR Data Acquired With ALOS-PALSAR. *Proc IEEE*, 100(10), pp. 2851-2860.
- [6] Chen S.W., Sato M., 2013. Tsunami Damage Investigation of Built-Up Areas Using Multitemporal Spaceborne Full Polarimetric SAR Images. *IEEE Trans Geosci Remote Sens*, 51(4), pp. 1985-1997.
- [7] Park S.E., Yamaguchi Y., Kim D., 2013. Polarimetric SAR remote sensing of the 2011 Tohoku earthquake using ALOS/PALSAR. *Remote Sens Environ*, 132, pp. 212-220.
- [8] Sato M., Chen S.W., Satake M., 2012. Polarimetric SAR Analysis of Tsunami Damage Following the March 11, 2011 East Japan Earthquake. *Proc IEEE*, 100(10), pp. 2861-2875.
- [9] Watanabe M., Motohka T., Miyagi Y., Yonezawa C., Shimada M., 2012. Analysis of Urban Areas Affected by the 2011 Off the Pacific Coast of Tohoku Earthquake and Tsunami With L-Band SAR Full-Polarimetric Mode. *IEEE Geosci Remote Sens Lett*, 9(3), pp. 472-476.
- [10] Guo H.D., Wang X.Y., Li X.W., Liu G., Zhang L., Yan S.Y., 2010. Yushu earthquake synergic analysis using multimodal SAR datasets. *Chinese Sci Bull*, 55(31), pp. 3499-3503.
- [11] Li X.W., Guo H.D., Zhang L., Chen X., Liang L., 2012. A New Approach to Collapsed Building Extraction Using RADARSAT-2 Polarimetric SAR Imagery. *IEEE Geosci Remote Sens Lett*, 9(4), pp. 677-681.
- [12] Zhao L., Yang J., Li P., Zhang L., Shi L., Lang F., 2013. Damage assessment in urban areas using post-earthquake airborne PolSAR imagery. *Int J Remote Sens*, 34(24), pp. 8952-8966.
- [13] Shen J.C., Xu X., Dong H., Gui R., Song C., 2015. Collapsed Building Extraction from Single Full Polarimetric SAR Image after Earthquake. *Sci Technol Eng*, 15(14), pp. 86-91.
- [14] Lee J.S., Schuler D.L., Ainsworth T.L., 2000. Polarimetric SAR data compensation for terrain azimuth slope variation. *IEEE Trans Geosci Remote Sens*, 38(5), pp. 2153-2163.
- [15] Yamaguchi Y., Moriyama T., Ishido M., Yamada H., 2005. Four-component scattering model for polarimetric SAR image decomposition. *IEEE Trans Geosci Remote Sens*, 43(8), pp. 1699-1706.
- [16] Lee J.S., Grunes M.R., Ainsworth T.L., Li-Jen D., Schuler D.L., Cloude S.R., 1999. Unsupervised classification using polarimetric decomposition and the complex Wishart classifier. *IEEE Trans Geosci Remote Sens*, 37(5), pp. 2249-2258.